

## Accepted Manuscript

Mesoporous immunosensor applied to zearalenone determination in *Amaranthus cruentus* seeds

Matías Regiart, Odil Fernández, Ana Vicario, Jhonny Villarroel-Rocha, Karim Sapag, Germán A. Messina, Julio Raba, Franco A. Bertolino



PII: S0026-265X(18)30302-3  
DOI: doi:[10.1016/j.microc.2018.05.051](https://doi.org/10.1016/j.microc.2018.05.051)  
Reference: MICROC 3200  
To appear in: *Microchemical Journal*  
Received date: 15 March 2018  
Revised date: 17 May 2018  
Accepted date: 28 May 2018

Please cite this article as: Matías Regiart, Odil Fernández, Ana Vicario, Jhonny Villarroel-Rocha, Karim Sapag, Germán A. Messina, Julio Raba, Franco A. Bertolino , Mesoporous immunosensor applied to zearalenone determination in *Amaranthus cruentus* seeds. *Microc* (2017), doi:[10.1016/j.microc.2018.05.051](https://doi.org/10.1016/j.microc.2018.05.051)

This is a PDF file of an unedited manuscript that has been accepted for publication. As a service to our customers we are providing this early version of the manuscript. The manuscript will undergo copyediting, typesetting, and review of the resulting proof before it is published in its final form. Please note that during the production process errors may be discovered which could affect the content, and all legal disclaimers that apply to the journal pertain.

**Mesoporous immunosensor applied to zearalenone determination in *Amaranthus  
cruentus* seeds**

Matías Regiart<sup>a</sup>, Odil Fernández<sup>b</sup>, Ana Vicario<sup>a</sup>, Jhonny Villarroel-Rocha<sup>c</sup>, Karim Sapag<sup>c</sup>,  
Germán A. Messina<sup>a</sup>, Julio Raba<sup>a</sup>, Franco A. Bertolino<sup>a\*</sup>

<sup>a</sup> INQUISAL-CONICET. Departamento de Química, Universidad Nacional de San Luis.  
Chacabuco 917, D5700BWS, San Luis, Argentina.

<sup>b</sup> Facultad de Ingeniería y Ciencias Agropecuarias, Universidad Nacional de San Luis.  
Ruta Provincial N° 55, D5730, Villa Mercedes, San Luis, Argentina.

<sup>c</sup> INFAP-CONICET. Laboratorio de Sólidos Porosos, Universidad Nacional de San Luis.  
Ejercito de los Andes 950, D5700BWS, San Luis, Argentina.

\*Author to whom correspondence should be addressed: bertolin@unsl.edu.ar (F.A. Bertolino), (Tel/Fax) +54 (0266) 444 6765. INQUISAL. Universidad Nacional de San Luis. Chacabuco 917. D5700BWS, San Luis, Argentina.

## Abstract

We describe an electrochemical immunosensor for zearalenone (ZEA) determination in *Amaranthus cruentus* seeds by an enzyme immunoassay sandwich type. The device is based on a screen-printed carbon electrode (SPCE) modified with amino mesoporous silica (MCM-41) synthesized with  $\text{Fe}_2\text{O}_3$  *in situ*. Mesoporous material enlarges the surface available for anti-ZEA antibodies immobilization. SPCE/MCM-41- $\text{Fe}_2\text{O}_3$  was characterized by scanning electron microscopy, energy dispersive X-ray spectroscopy, and cyclic voltammetry.

ZEA in the sample previously pretreated was recognized and captured by anti-ZEA on SPCE/MCM-41- $\text{Fe}_2\text{O}_3$ . Then, the horseradish peroxidase (HRP)-conjugated anti-ZEA-antibody was added, and the substrate solution ( $\text{H}_2\text{O}_2$  + 4-terbutylcatechol (4-TBC)) reacted with the HRP that catalyzed the oxidation of 4-TBC to 4-terbutylbenzoquinone (TBQ). Finally, the enzymatic product was detected at  $-100$  mV, and the current was proportional to the ZEA present in the sample.

The calibration plot exhibited a linear range from  $1.88$  to  $45$  ng mL $^{-1}$ , and the limit of detection was  $0.57$  ng mL $^{-1}$  ( $r^2 = 0.998$ ). The coefficient of variation inter- and intra assay was below 6%. Our method achieved a good selectivity, stability and reproducibility for ZEA detection in *A. cruentus* seeds.

**Keywords:** Electrochemical; immunosensor; mesoporous silica; zearalenone; *Amaranthus cruentus* seeds

## 1. Introduction

Zearalenone (ZEA, also known as F-2 toxin) is a mycotoxin produced by several *Fusarium* species [1]. ZEA was found in cereal grains, feedstuff, and manufactured foods, through fungal contamination before/after harvest, during grain processing and storage [2, 3]. ZEA is considered as an endocrine-disrupting compound (EDC), shows estrogen-like activity and can cause serious damage to the human reproductive systems. Despite its non-steroidal structure, ZEA and its metabolites compete with endogenous steroids, activate estrogen receptors, and disrupt steroid synthesis and metabolism [4,5]. Its hydroxylated metabolite  $\alpha$ -zearalenol has even higher estrogenic potency.

EDCs are any environmental pollutant chemical that, once incorporated into an organism, affects the hormonal balance of several species including humans [6]. Moreover, in higher concentrations ZEA cause several health disorders such as hepatotoxicity, hematological toxicity, genotoxicity, immunotoxicity and neurotoxicity, and was classified as group III carcinogen by the International Agency for Research on Cancer [7]. In order to prevent and improve the public health, the tolerable levels of ZEN for different agricultural products have been established by national and international organizations. In Argentina, the allowed maximum level of ZEA is  $200 \mu\text{g kg}^{-1}$  in maize, and in the European Union is  $100 \mu\text{g kg}^{-1}$  for cereals and  $350 \mu\text{g kg}^{-1}$  for unprocessed maize [8,9].

Thus, developing a sensitive detection method to ensure food safety, as well as consumer's health is vital. Various analytical techniques have been reported for the ZEA quantitative detection in several cereals, including high performance liquid chromatography (HPLC) - mass spectrometry [10-12], lateral flow immunoassays [13], aptasensors [14], biosensors [15], fluorescence [16], surface plasmon resonance (SPR) [17], and enzyme linked immunosorbent assays [18-20]. These procedures can detect ZEA with high

robustness and accuracy. However, such methods require expensive equipment, complicated sample preparation, and specialized staff.

In recent years, immunoassay techniques, which are based on the highly specific molecular recognition of antigens by antibodies, have become an important analytical method in several fields [21, 22]. Furthermore, many electrochemical immunosensors for food safety analysis were developed, due to the electrochemical methods provides several useful properties including the required detection limit, fast analysis times, low cost of the instrumentation, low sample and reagent consumption, portability, ease of use, high sensitivity and selectivity [23, 24]. Screen-printing electrodes is one of the most promising approaches towards simple, rapid and inexpensive immunosensors production, and has advantages of flexibility design, automation process, and good reproducibility [25].

In the last years, different materials have been incorporated into electrochemical immunosensors as immobilization platforms for the specific immunogenic reagents. Porous silica materials have many advantages, such as the increase of the surface to volume ratio that increases interactions between the ZEA and anti-ZEA antibodies, and therefore low the detection limit [26]. We synthesized mesoporous silica (MCM-41) with  $\text{Fe}_2\text{O}_3$  *in situ*, functionalized with amino groups, characterized (an increased surface and uniform porous) and used as immobilization platform for the anti-ZEA antibody.

We describe the first electrochemical immunosensor for ZEA determination in *A. cruentus* seeds. This device was built on a screen-printed carbon electrode (SPCE) modified with MCM-41- $\text{Fe}_2\text{O}_3$ , functionalized with anti-ZEA antibodies. SPCE/MCM-41- $\text{Fe}_2\text{O}_3$  was characterized by scanning electron microscopy (SEM), energy dispersive X-ray spectroscopy (EDS), and cyclic voltammetry (CV). ZEA in the sample previously pretreated was recognized and captured by anti-ZEA on SPCE/MCM-41- $\text{Fe}_2\text{O}_3$ . Then, the horseradish

peroxidase (HRP)-conjugated anti-ZEA-antibody was added, and the substrate solution ( $\text{H}_2\text{O}_2$  + 4-terbutylcatechol (4-TBC)) reacted with the HRP that catalyzed the oxidation of 4-TBC to 4-terbutylbenzoquinone (TBQ). Finally, the enzymatic product was detected at -100 mV, and the obtained current was proportional to ZEA present in the sample. Our method exhibited good selectivity, stability and reproducibility for ZEA detection to ensure food safety, as well as consumer's health.

## 2. Materials and methods

### 2.1. Reagents

All reagents used were of analytical reagent grade. Glutaraldehyde (25% aqueous solution), methanol, ethanol, toluene, tetraethyl orthosilicate  $\text{SiC}_8\text{H}_{20}\text{O}_4$  (TEOS 98%) as the silica source, cetyltrimethylammonium bromide  $\text{C}_{16}\text{H}_{33}\text{N}(\text{CH}_3)_3\text{Br}$  (CTAB) as the surfactant, and 3-aminopropyl triethoxysilane (3-APTES) were purchased from Merck (Darmstadt, Germany). Iron(III) nitrate nonahydrate  $\text{Fe}(\text{NO}_3)_3 \cdot 9\text{H}_2\text{O}$  was acquired from Anedra. Bovine serum albumin (BSA), and HCl (37% w/w) were purchased from Sigma-Aldrich (St. Louis, MO, USA). AgraQuant<sup>®</sup> Zearalenone Plus Test kit licensed by Roemer Labs<sup>®</sup>, Inc. (USA). Anti-Zearalenone (Anti-ZEA) antibody (mouse monoclonal [11C9] ab42123) to ZEA was purchased from abcam (USA), and used according to the manufacturer's instructions. *A. cruentus* var. Candil seeds samples were provided by the Universidad Nacional de Río Cuarto (Río Cuarto, Córdoba, Argentina). All the other employed reagents were of analytical grade and were used without further purification. Aqueous solutions were prepared by using purified water from a Milli-Q system.

### 2.2. Apparatus

Amperometric detection was performed with a BAS LC-4C electrochemical detector (Bioanalytical Systems, Inc. West Lafayette, IN, USA). A SPCE made up of three electrodes was used. A silver ink as pseudo-reference electrode, a graphite ink as auxiliary electrode and, a graphite ink circular ( $\varnothing = 3$  mm) with and without modifications as working electrode were used for all the measurements (DropSens, Llanera, Asturias, Spain).

The iron loading of the MCM-41-Fe<sub>2</sub>O<sub>3</sub> was determined by atomic absorption spectrometry (SpectrAA 50, Varian). Infrared (FTIR) spectroscopic measurement was obtained in an LPHA FT-IR Spectrometer (Bruker), in a region from 2000 to 500 cm<sup>-1</sup>. Scanning Electron Microscopy (SEM) images were taken on a FEI “Quanta 200”. Textural characterization was carried out by N<sub>2</sub> adsorption–desorption isotherms at 77 K using a manometric adsorption equipment (ASAP 2000, Micromeritics), where the samples were previously degassed at 150 °C for 20 h, up to a residual pressure smaller than 2 Pa.

All solutions and reagent temperatures were conditioned before the experiment using a Vicking Masson II laboratory water bath (Vicking SRL, Buenos Aires, Argentina). Absorbance was detected by Bio-Rad Benchmark microplate reader (Japan) and Beckman DU 520 general UV/VIS spectrophotometer. All pH measurements were made with an Orion Expandable Ion Analyzer (Orion Research Inc., Cambridge, MA, USA) Model EA 940 equipped with a glass combination electrode (Orion Research Inc).

### 2.3. Synthesis and functionalization of amino MCM-41-Fe<sub>2</sub>O<sub>3</sub>

MCM-41-Fe<sub>2</sub>O<sub>3</sub> was synthesized by direct-synthesis method at room temperature without hydrothermal treatment according to a modification of the procedure reported by Barrera et al. (2011) [27]. The reagents used were CTAB (cetyltrimethylammonium bromide, C<sub>16</sub>H<sub>33</sub>N(CH<sub>3</sub>)<sub>3</sub>Br) as the surfactant, TEOS (Tetraethyl orthosilicate, SiC<sub>8</sub>H<sub>20</sub>O<sub>4</sub>) as the silica

source, Iron(III) nitrate nonahydrate ( $\text{Fe}(\text{NO}_3)_3 \cdot 9\text{H}_2\text{O}$ ) as the iron source, NaOH as the catalyst and water as the solvent. The molar ratio used for the MCM-41- $\text{Fe}_2\text{O}_3$  preparation were: 0.12CTAB:1TEOS:0.047Fe:0.6NaOH:100 $\text{H}_2\text{O}$ . First, CTAB was suspended in deionized water and then mixed with an aqueous solution of 1 mol  $\text{L}^{-1}$  NaOH with vigorous stirring until a transparent solution was obtained. Subsequently, the TEOS and an aqueous solution of  $\text{Fe}(\text{NO}_3)_3 \cdot 9\text{H}_2\text{O}$  were added drop-wise to this solution and kept under vigorous stirring for 24 h at room temperature. Then, the solids obtained were filtrated, washed with abundant deionized water until reaching a conductivity value smaller than 10  $\mu\text{S cm}^{-1}$ , dried at 60 °C for 12 h and calcined at 550 °C for 6 h at a heating rate of 1 °C  $\text{min}^{-1}$ .

Amino functionalization was prepared according to the following procedure. Firstly, 1 mL of APTES (50 mmol  $\text{L}^{-1}$ ) was introduced to 1 g MCM-41- $\text{Fe}_2\text{O}_3$ , and was stirring vigorously. Then, the mixture was refluxed at 80 °C for 6 h. Finally, the MCM-41- $\text{Fe}_2\text{O}_3$  was washed with toluene followed by ethanol, and dried at 60 °C for 12 h. Amino-MCM-41- $\text{Fe}_2\text{O}_3$  was resuspended in distilled water and preserved at 4 °C stable for at least 3 months.

#### 2.4. Anti-ZEA immobilization in the amino MCM-41- $\text{Fe}_2\text{O}_3$

The immobilization process of the anti-ZEA antibodies follow the next steps; 1 mL of 5% w/w glutaraldehyde solution (0.10 mol  $\text{L}^{-1}$  sodium phosphate buffer, pH 8.00) was put in contact with 15  $\mu\text{L}$  amino-MCM-41- $\text{Fe}_2\text{O}_3$  over the SPCE, for 2 h at room temperature. After three washes with 0.01 mol  $\text{L}^{-1}$  phosphate buffer saline (PBS) pH 7.00, 250  $\mu\text{L}$  of antibody preparation (dilution 1/500 -concentration previously evaluated- in 0.01 mol  $\text{L}^{-1}$  PBS pH 7.00) was coupled to the residual aldehyde groups for 12 h at 4 °C. The immobilized antibody preparation was finally washed three times with PBS (0.01 mol  $\text{L}^{-1}$  pH 7.00) and



stored in the same buffer at 4 °C. Anti-ZEA/MCM-41-Fe<sub>2</sub>O<sub>3</sub> was perfectly stable for at least 1 month (Scheme 1).

## 2.5. Sample preparation

Zearalenone was detected for the first time as a natural contaminant in two samples of *A. cruentus* seeds provided by the Universidad Nacional de Río Cuarto (Río Cuarto, Córdoba, Argentina). Although there are more than fifty species of *Amaranthus*, the main species identified and with the possibility of becoming grain crops are: *A. cruentus*, *A. audatus*, and *A. hypochondriacus*.

*A. Cruentus* is a pseudocereal with very small seeds, its cultivation and consumption is of great importance because of its high nutritional value, so like cereals, is susceptible to fungi toxigenic development. Firstly, the seeds were washed with double distilled water. Representative samples (approximately 10 g) were ground until a fine particle size. The powder was mixed with ethanol/H<sub>2</sub>O (2:1) solution for 2 h at room temperature. The extract was filtered through a Whatman #1 filter. Finally, several dilutions in 0.01 mol L<sup>-1</sup> PBS pH 7.00 were prepared and stored at 4 °C until use.

## 2.6. Analytical procedure for ZEA quantification in *A. cruentus* seeds

The procedure for the ZEA determination involves the following steps. Firstly, the electrochemical immunosensor was exposed to 1% BSA in 0.01 mol L<sup>-1</sup> PBS pH 7.00 to block the unspecific binding by a 5 min treatment at room temperature and then was rinsed with 0.01 mol L<sup>-1</sup> PBS pH 7.00 for 2 min.

After that, the *A. cruentus* seeds samples (previously diluted 10-fold with 0.01 mol L<sup>-1</sup> PBS pH 7.00), was put in contact with the device for 5 min at room temperature. So, ZEA

was recognized and captured by anti-ZEA immobilized on the MCM-41-Fe<sub>2</sub>O<sub>3</sub>. In the next step, the immunosensor was washed with 0.01 mol L<sup>-1</sup> PBS pH 7.00 for 2 min to remove sample excess. Later, HRP-anti-ZEA-antibody (diluted 1:500 with 0.01 mol L<sup>-1</sup> PBS pH 7.00) was added for 5 min, following by a washing step (2 min). Finally, the substrate solution (1 mmol L<sup>-1</sup> H<sub>2</sub>O<sub>2</sub> + 1 mmol L<sup>-1</sup> 4-TBC in 0.01 mol L<sup>-1</sup> phosphate-citrate buffer pH 5.00) reacted with the HRP that catalyzed the oxidation of 4-TBC to TBQ. The enzymatic product was detected at -100 mV, and the current was proportional to the ZEA present in the sample (Scheme 2).

Then, the electrochemical immunosensor was exposed to a desorption buffer (0.1 mol L<sup>-1</sup> citrate-HCl pH 2.00) for 5 min and then was rinsed with 0.01 mol L<sup>-1</sup> PBS pH 7.00 for 2 min. This treatment was carried out in order to desorb the immune-complex and start with a new analysis. The sensor could be used with no significant loss of sensitivity for 20 days, whereas its useful lifetime was one month with a sensitivity decrease of 15%. When not in use the immunosensor was storage in 0.01 mol L<sup>-1</sup> PBS pH 7.00 at 4 °C.

### 3. Results and discussion

#### 3.1. Textural characterization of MCM-41-Fe<sub>2</sub>O<sub>3</sub>

The specific surface area (SBET) of materials under study was estimated by the Brunauer, Emmet and Teller (BET) method [28], using the adsorption data in the range of relative pressures from 0.05 to 0.13. The total pore volume (VTP) was determined by the Gurvich's rule at a relative pressure of 0.985. The micropore volume (V<sub>μP</sub>) and the narrow mesopore volume (VNMP) were calculated by the αS-plot method [29] using the LiChrospher Si-1000 macroporous silica gel [30] as the reference adsorbent. The pore size distribution of the MCM-41-Fe<sub>2</sub>O<sub>3</sub> sample was obtained by NLDFT method with adsorption

branch data using the kernel for cylindrical pore geometry “N<sub>2</sub> at 77 K on silica, cylindrical pore, NLDFT adsorption” [31] included in ASiQwin software, v. 2.0 (Quantachrome).

Fig. 1a shows the FT-IR spectrum of the MCM-41-Fe<sub>2</sub>O<sub>3</sub> sample (which present an iron load of 5.8 wt. %). In this spectrum, the bands at 660 cm<sup>-1</sup> and 960 cm<sup>-1</sup> correspond to the Si-O-Fe species. In addition, the band observed at 580 cm<sup>-1</sup> is related to the stretching vibration mode of Fe-O. The texture of the MCM-41-Fe<sub>2</sub>O<sub>3</sub> sample was studied by means of N<sub>2</sub> adsorption-desorption at 77 K, as shown in Fig. 1b. According to the IUPAC classification [32], this sample exhibit a Type I(b) isotherm characteristic of porous materials which present supermicropores and narrow mesopores, as shown in Fig. 1c, where a bi-modal pore size distribution (with micropores and mesopores sizes around 1.3 nm and 2.5 nm, respectively) is observed. In addition, in the N<sub>2</sub> adsorption isotherm (Fig. 1b), it is possible to observe a quickly increase the N<sub>2</sub> adsorbed amount at high relative pressures ( $p/p_0 > 0.9$ ) corresponding to the N<sub>2</sub> adsorption on larger mesopores or narrow macropores (i.e. interparticle porosity of the Fe<sub>2</sub>O<sub>3</sub> agglomerates observed in the SEM micrographs). The Fe/MCM-41-Fe<sub>2</sub>O<sub>3</sub> sample have the following textural properties: SBET: 660 m<sup>2</sup> g<sup>-1</sup>, V<sub>μP</sub>: 0.04 cm<sup>3</sup> g<sup>-1</sup>, VNMP: 0.24 cm<sup>3</sup> g<sup>-1</sup> and VTP: 0.48 cm<sup>3</sup> g<sup>-1</sup>.

The morphology of the pure MCM-41 and MCM-41-Fe<sub>2</sub>O<sub>3</sub> samples are show in SEM (Fig. 2). The particles of both samples exhibited an approximate particle size of 1 μm, but the MCM-41-Fe<sub>2</sub>O<sub>3</sub> present a surface roughness compared to pure MCM-41, which may be related to the Fe<sub>2</sub>O<sub>3</sub> deposited (as agglomerates) outside of the MCM-41 structure.

### 3.2. Electrochemical characterization of MCM-41-Fe<sub>2</sub>O<sub>3</sub>

MCM-41 was compared with the MCM-41-Fe<sub>2</sub>O<sub>3</sub> in order to analyze the electrochemical behaviour of both mesoporous silica materials over the SPCE. As can be seen in Fig. 3, CVs of 1 mmol L<sup>-1</sup> K<sub>3</sub>[Fe(CN)<sub>6</sub>]/K<sub>4</sub>[Fe(CN)<sub>6</sub>] in 0.1 mol L<sup>-1</sup> KCl (pH 6.50) solution were performed. K<sub>3</sub>[Fe(CN)<sub>6</sub>]/K<sub>4</sub>[Fe(CN)<sub>6</sub>] couple is a convenient and valuable tool to examine the characteristics of the modified surface. The figure shows the CVs of unmodified SPCE (red line), modified with MCM-41 (black line), and MCM-41-Fe<sub>2</sub>O<sub>3</sub> (blue line), from -300 mV to +900 mV at a 75 mV s<sup>-1</sup> scan rate. CVs well defined and characteristics of a diffusion controlled redox process were observed.

As showed in the previous figure, the current intensities of the oxidation and reduction processes decrease when the electrode is modified with MCM-41. This behaviour occurs because the silica blocks the SPCE surface decreasing the current of the electrochemical couple. On the other hand, it can be observed that the behaviour of the silica modified with Fe<sup>+3</sup> (MCM-41-Fe<sub>2</sub>O<sub>3</sub>) maintains and even improves the current of the electrochemical couple, because the presence of Fe<sub>2</sub>O<sub>3</sub> improves the electronic transfer, so no loss of sensitivity in the detection was showed.

### 3.3. Optimization of experimental variables

Relevant studies of experimental variables that affect the electrochemical immunosensor performance for ZEA determination in *A. cruentus* seeds were studied. For this purpose, a ZEA standard solution of 15 ng mL<sup>-1</sup> was employed.

An important parameter to consider in the immunosensor optimization procedure is the pH. As shown in Fig. 4 a, the rate of enzymatic response was studied in the pH range from 2.00 to 7.00. As can be seen, the current increased until pH 5.00 and then remained constant until pH 7.00. So, the maximum value of activity was at 0.01 mol L<sup>-1</sup> phosphate-

citrate buffer pH 5.00. Another relevant parameter is the enzyme conjugate concentration. This factor was evaluated using HRP-anti-ZEA in 1:100, 1:250, 1:500, 1:750, 1:1000, and 1:1500. The response rate increased with concentrated solutions until 1:500, where can be observed an increase in the sensitivity, later insignificant differences can be noted when the solutions of 1:250 and 1:100 were used. So, a HRP-conjugated concentration of 1:500 was used (Fig. 4 b).

As can be seen in Fig. 4 c, the effect of varying  $\text{H}_2\text{O}_2$  concentration was studied from 0.1 to 1.5  $\text{mmol L}^{-1}$  on the electrochemical immunosensor response. The optimum  $\text{H}_2\text{O}_2$  concentration was 1  $\text{mmol L}^{-1}$ . Finally, the 4-TBC concentration was analyzed between 0.1 to 1.5  $\text{mmol L}^{-1}$ . A 1  $\text{mmol L}^{-1}$  4-TBC concentration was used as optimum (Fig. 4 d). As seen for ZEA quantification, small reactive volumes and concentrations were required; this point is very important because the cost of reagents can be very expensive. Therefore, it has always been an aim to reduce reagents volume and increase sensitivity in all biological assays.

### 3.4. Immunosensor analytical behavior

A calibration curve with ZEA standard solutions for the electrochemical immunosensor was described according to the following equation:  $\Delta I \text{ (nA)} = 15.18 + 19.33 [\text{ZEA}] \text{ (ng mL}^{-1}\text{)}$  with a correlation coefficient ( $r^2$ ) of 0.998 (Fig. 5). A linear relation was observed between the concentration range from 1.88 to 45  $\text{ng mL}^{-1}$ . The detection (LOD) and quantification (LOQ) limits were determined according to the IUPAC recommendations [37], achieving values of 0.57 and 1.73  $\text{ng mL}^{-1}$ , respectively.

The coefficient of variation (CV%) for the determination of 15  $\text{ng mL}^{-1}$  ZEA was 4.67% ( $n=6$ ). The within-assay precision was tested with five measurements in the same run for each control. These series of five measurements were repeated for three consecutive days

to estimate between-assay precision. The CV% within-assay values was 5.15% and the between assay values was 5.91%. Moreover, the electrochemical immunosensor was compared with an ELISA for ZEA quantification in four *A. cruentus* seeds samples under the conditions previously described. The results demonstrated that both methods were statistically equal at a confidence level of 90% (Table 1).

Moreover, the developed method was compared with other immunosensors for ZEA determination (Table 2). As can be seen, our analytical method has significant advantages, and this is the first electrochemical immunosensor for ZEA detection in *A. cruentus* seeds. The electrochemical immunosensor uses amperometry as detection technique, which offers high sensitive determinations in short analysis time, with a low consumption of reagents and samples, including a low cost equipment. In addition, our device incorporates the amino functionalized MCM-41 as immobilization platform for the anti-ZEA antibodies, which provides high specificity. Furthermore, the achieved limit of detection is lower than that obtained by the ELISA.

#### 4. Conclusions

This article described the development of an electrochemical immunosensor for ZEA quantitative detection in *A. cruentus* seeds samples. Our analytical method is based on the anti-ZEA covalently immobilization on amino functionalized MCM-41-Fe<sub>2</sub>O<sub>3</sub> over a SPCE. The assay time employed (less than 20 min) was shorter than the used for ELISA test kit (90 min). The immunosensor offered several advantages like high stability, selectivity and sensitivity. In conclusion, our device is an excellent analytical tool for the ZEA quantification in *A. cruentus* seeds avoiding health human problems and serious economic losses.

## Acknowledgements

The authors wish to thank the financial support from Universidad Nacional de San Luis (UNSL), Instituto de Química de San Luis (INQUISAL), Instituto de Física Aplicada (INFAP), Consejo Nacional de Investigaciones Científicas y Técnicas (CONICET). PICT-2016-0942, PICT-2015-2246, PICT-2014-1184 (ANPCyT-FONCyT), PROICO-2-1816-22/Q632 (UNSL), PIP-11220150100004CO (CONICET), *A. cruentus* var. Candil seeds samples were provided by Ing. Guillermo Peiretti, Universidad Nacional de Río Cuarto (Río Cuarto, Córdoba, Argentina).

## References

- [1] J. Liu, Y. Hu, G. Zhu, X. Zhou, L. Jia, T. Zhang, Highly sensitive detection of zearalenone in feed samples using competitive surface-enhanced Raman scattering immunoassay, *J. Agric. Food Chem.* 33 (2014) 8325-8332.
- [2] A.B. Serrano, G. Font, J. Maes, E. Ferrer, Dispersive liquid-liquid microextraction for the determination of emerging *Fusarium* mycotoxins in water, *Food Anal. Method.* 9 (2016) 856-862.
- [3] H. Zheng, H. Yi, W. Lin, H. Dai, Z. Hong, Y. Lin, X. Li, A dual-amplified electrochemiluminescence immunosensor constructed on dual-roles of rutile TiO<sub>2</sub> mesocrystals for ultrasensitive zearalenone detection, *Electrochim. Acta* 260 (2018) 847-854.
- [4] L. Li, H. Chen, X. Lv, M. Wang, X. Jiang, Y. Jiang, H. Wang, Y. Zhao, L. Xia, Paper-based immune-affinity arrays for detection of multiple mycotoxins in cereals, *Anal. Bioanal. Chem.* 410 (2018) 2253-2262.
- [5] I. Lhotská, B. Gajdošová, P. Solich, D. Šatínský, Molecularly imprinted vs. reversed-phase extraction for the determination of zearalenone: a method development and critical comparison of sample clean-up efficiency achieved in an on-line coupled SPE chromatography system, *Anal. Bioanal. Chem.* (2018) 1-9 <https://doi.org/10.1007/s00216-018-0920-2>.
- [6] J. Fink-Gremmels, H. Malekinejad, Clinical effects and biochemical mechanisms associated with exposure to the mycoestrogen zearalenone, *Anim. Feed Sci. Technol.* 137 (2007) 326-41.
- [7] X. Zhang, S. A. Eremin, K. Wen, X. Yu, C. Li, Y. Ke, H. Jiang, J. Shen, Z. Wang, Fluorescence polarization immunoassay based on a new monoclonal antibody for the



detection of the zearalenone class of mycotoxins in maize, *J. Agric. Food Chem.* 65 (2017) 2240-2247.

[8] B. Zhang, Y. Pan, H. Chen, T. Liu, H. Tao, Y. Tian, Stabilization of starch based microgel-lysozyme complexes using a layer-by-layer assembly technique, *Food Chem.* 214 (2017) 213-217.

[9] B. Zhang, H. Tao, X. Niu, S. Li, H.Q. Chen, Lysozyme distribution, structural identification, and in vitro release of starch-based microgel-lysozyme complexes, *Food Chem.* 227 (2017) 137-141.

[10] A.L. Manizan, M. Oplatowska-Stachowiak, I. Piro-Metayer, K. Campbell, R. Koffi-Nevry, C. Elliott, D. Akaki, D. Montet, C. Brabet, Multi-mycotoxin determination in rice, maize and peanut products most consumed in Cote d' Ivoire by UHPLC-MS/MS, *Food Control* 87 (2018) 22-30.

[11] Z. Han, K. Jiang, Z. Fan, J.D. Di Mavungu, M. Dong, W. Guo, K. Fan, K. Campbell, Z. Zhao, Y. Wu, Multi-walled carbon nanotubes-based magnetic solid-phase extraction for the determination of zearalenone and its derivatives in maize by ultra-high performance liquid chromatography-tandem mass spectrometry, *Food Control* 79 (2017) 177-184.

[12] X. Li, B. Liu, F. Wang, X. Ma, Z. Li, D. Guo, Y. Wang, F. Wan, L. Deng, S. Zhang, Determination of sixteen mycotoxins in maize by ultra-high performance liquid chromatography–tandem mass Spectrometry, *Anal. Letters* 51 (2017) 702-716.

[13] Y. Chen, Q. Chen, M. Han, J. Zhou, L. Gong, Y. Niu, Y. Zhang, L. He, L. Zhang Development and optimization of a multiplex lateral flow immunoassay for the simultaneous determination of three mycotoxins in corn, rice and peanut, *Food Chem.* 213 (2016) 478-484.

- [14] Z. Wu, E. Xu, M.F.J. Chughtai, Z. Jin, J. Irudayaraj, Highly sensitive fluorescence sensing of zearalenone using a novel aptasensor based on upconverting nanoparticles, *Food Chem.* 230 (2017) 673-680.
- [15] A.V. Orlov, A.G. Burenin, N.G. Massarskaya, A.V. Betin, M.P. Nikitin, P.I. Nikitin, Highly reproducible and sensitive detection of mycotoxins by label-free biosensors, *Sensor. Actuat. B-Chem.* 246 (2017) 1080-1084.
- [16] X. Zhang, Q. Tang, T. Mi, S. Zhao, K. Wen, L. Guo, J. Mi, S. Zhang, W. Shi, J. Shen, Y. Ke, Z. Wang, Dual-wavelength fluorescence polarization immunoassay to increase information content per screen: Applications for simultaneous detection of total aflatoxins and family zearalenones in maize, *Food Control* 87 (2018) 100-108.
- [17] Md.Z. Hossain, C.M. Maragos, Gold nanoparticle-enhanced multiplexed imaging surface plasmon resonance (iSPR) detection of *Fusarium* mycotoxins in wheat, *Biosens. Bioelectron.* 101 (2018) 245-252.
- [18] F. Zhao, Q. Shen, H. Wang, X. Han, Z. Yang, Development of a rapid magnetic bead-based immunoassay for sensitive detection of zearalenone, *Food Control* 79 (2017) 227-233.
- [19] G. Dong, Y. Pan, Y. Wang, S. Ahmed, Z. Liu, D. Peng, Z. Yuan, Preparation of a broad-spectrum anti-zearalenone and its primary analogues antibody and its application in an indirect competitive enzyme-linked immunosorbent assay, *Food Chem.* 247 (2018) 8-15.
- [20] O.D. Hendrickson, J.O. Chertovich, A.V. Zherdev, P.G. Sveshnikov, B.B. Dzantiev, Ultrasensitive magnetic ELISA of zearalenone with pre-concentration and chemiluminescent detection, *Food Control* 84 (2018) 330-338.

[21] N. Liu, D. Nie, Z. Zhao, X. Meng, A. Wu, Ultrasensitive immunoassays based on biotin–streptavidin amplified system for quantitative determination of family zearalenones, *Food Control* 57 (2015) 202-209.

[22] Y. Huang, Y. Xu, Q. He, J. Chu, B. Du, J. Liu, Determination of zearalenone in corn based on a biotin-avidin amplified enzyme-linked immunosorbent assay, *Food Agric. Immunol.* 25 (2014) 186-199.

[23] W.I. Riberi, L.V. Tarditto, M.A. Zon, F.J. Arévalo, H. Fernández, Development of an electrochemical immunosensor to determine zearalenone in maize using carbon screen printed electrodes modified with multi-walled carbon nanotubes/polyethyleneimine dispersions, *Sensor. Actuat. B-Chem.* 254 (2018) 1271-1277.

[24] W. Xu, Y. Qing, S. Chen, J. Chen, Z. Qin, J.F. Qiu, C.R. Li, Electrochemical indirect competitive immunoassay for ultrasensitive detection of zearalenone based on a glassy carbon electrode modified with carboxylated multi-walled carbon nanotubes and chitosan, *Microchim. Acta* 184 (2017) 3339-3347.

[25] Z. Taleat, A. Khoshroo, M. Mazloun-Ardakani, Screen-printed electrodes for biosensing: a review, *Microchim. Acta* 181 (2014) 865-891.

[26] M. Regiart, M. Rinaldi-Tosi, P.R. Aranda, F.A. Bertolino, J. Villarroel-Rocha, K. Sapag, G.A. Messina, J. Raba, M.A. Fernández-Baldo, Development of a nanostructured immunosensor for early and in situ detection of *Xanthomonas arboricola* in agricultural food production, *Talanta* 175 (2017) 535-541.

[27] D. Barrera, J. Villarroel-Rocha, K. Sapag, Non-hydrothermal synthesis of cylindrical mesoporous materials: Influence of the surfactant/silica molar ratio. *Adsorpt. Sci. Technol.* 29 (2011) 975-988.

- [28] S. Brunauer, P.H. Emmett, E. Teller, Adsorption of gasses in multimolecular layers. *J. Am. Chem. Soc.* 60 (1938) 309-319.
- [29] F. Rouquerol, J. Rouquerol, K.S.W. Sing, P. Llewellyn, G. Maurin, Adsorption by powders and porous solids: Principles, methodology and applications. Academic Press, San Diego, 2014.
- [30] M. Jaroniec, M. Kruk, J. Olivier, Standard nitrogen adsorption data for characterization of nanoporous silicas, *Langmuir* 15 (1999) 5410-5413.
- [31] A. Zukal, M. Thommes, J. Cejka, Synthesis of highly ordered MCM-41 silica with spherical particle. *Microporous Mesoporous Mater.* 104 (2007) 52-58.
- [32] M. Thommes, K. Kaneko, A.V. Neimark, J.P. Olivier, F. Rodriguez-Reinoso, J. Rouquerol, K.S.W. Sing, Physisorption of gases, with special reference to the evaluation of surface area and pore size distribution (IUPAC Technical Report). *Pure Appl. Chem.* 87 (2015) 1051-1069.
- [33] N.V. Panini, F.A. Bertolino, E. Salinas, G.A. Messina, J. Raba, Zearalenone determination in corn silage samples using an immunosensor in a continuous-flow/stopped-flow systems. *Biochem. Engineering Journal* 51 (2010) 7-13.
- [34] J.L. Urraca, E. Benito-Peña, C. Pérez-Conde, M.C. Moreno-Bondi, J.J. Pestka, Analysis of zearalenone in cereal and swine feed samples using an automated flow-through immunosensor. *J. Agric. Food Chem.* 53 (2005) 3338-3344.
- [35] N.V. Panini, E. Salinas, G.A. Messina, J. Raba, Modified paramagnetic beads in a microfluidic system for the determination of zearalenone in feedstuffs samples. *Food Chem.* 125 (2011) 791-796.

[36] M.H. Miguel, Á. López, A. Escarpa, Simplified calibration and analysis on screen-printed disposable platforms for electrochemical magnetic bead-based immunosensing of zearalenone in baby food samples. *Biosens. Bioelectron.* 25 (2010) 1755-1760.

[37] L.A. Currie, Nomenclature in evaluation of analytical methods including detection and quantification capabilities (IUPAC Recommendations 1995), *Pure Appl. Chem.* 67 (1995) 1699-1723.

## Figure captions

**Scheme 1.** Procedure for anti-ZEA-MCM-41-Fe<sub>2</sub>O<sub>3</sub> preparation.

**Scheme 2.** Procedure for ZEA quantification.

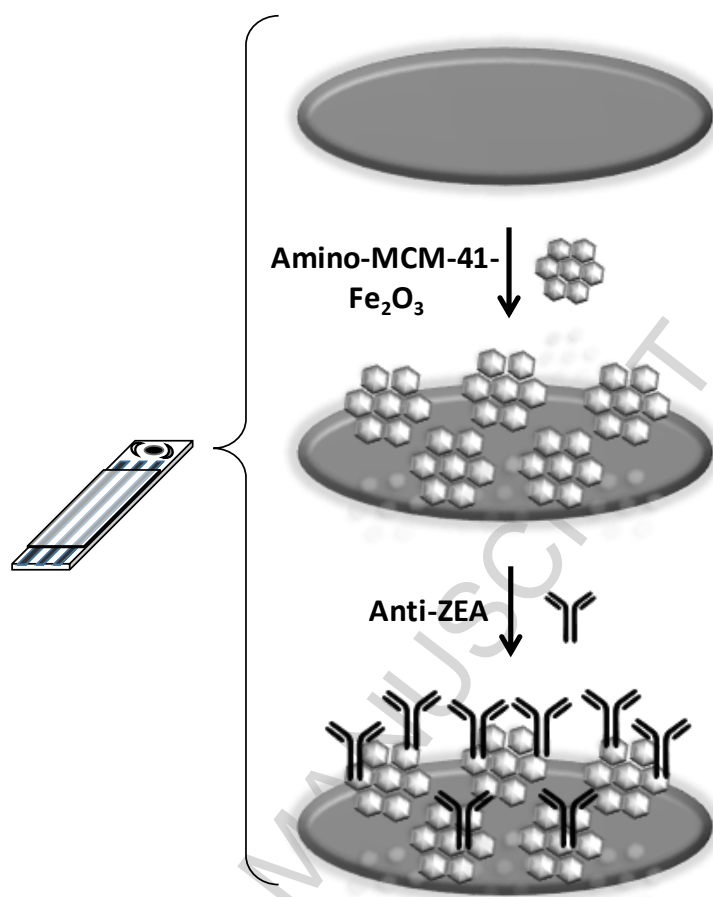
**Fig. 1.** Characterization of MCM-41-Fe<sub>2</sub>O<sub>3</sub>. a) FT-IR spectrum of MCM-41-Fe<sub>2</sub>O<sub>3</sub>, b) N<sub>2</sub> adsorption-desorption isotherm at 77 K, and (c) Pore size distribution of MCM-41-Fe<sub>2</sub>O<sub>3</sub>.

**Fig. 2.** SEM micrographs of (a) pure MCM-41, and (b) MCM-41-Fe<sub>2</sub>O<sub>3</sub>.

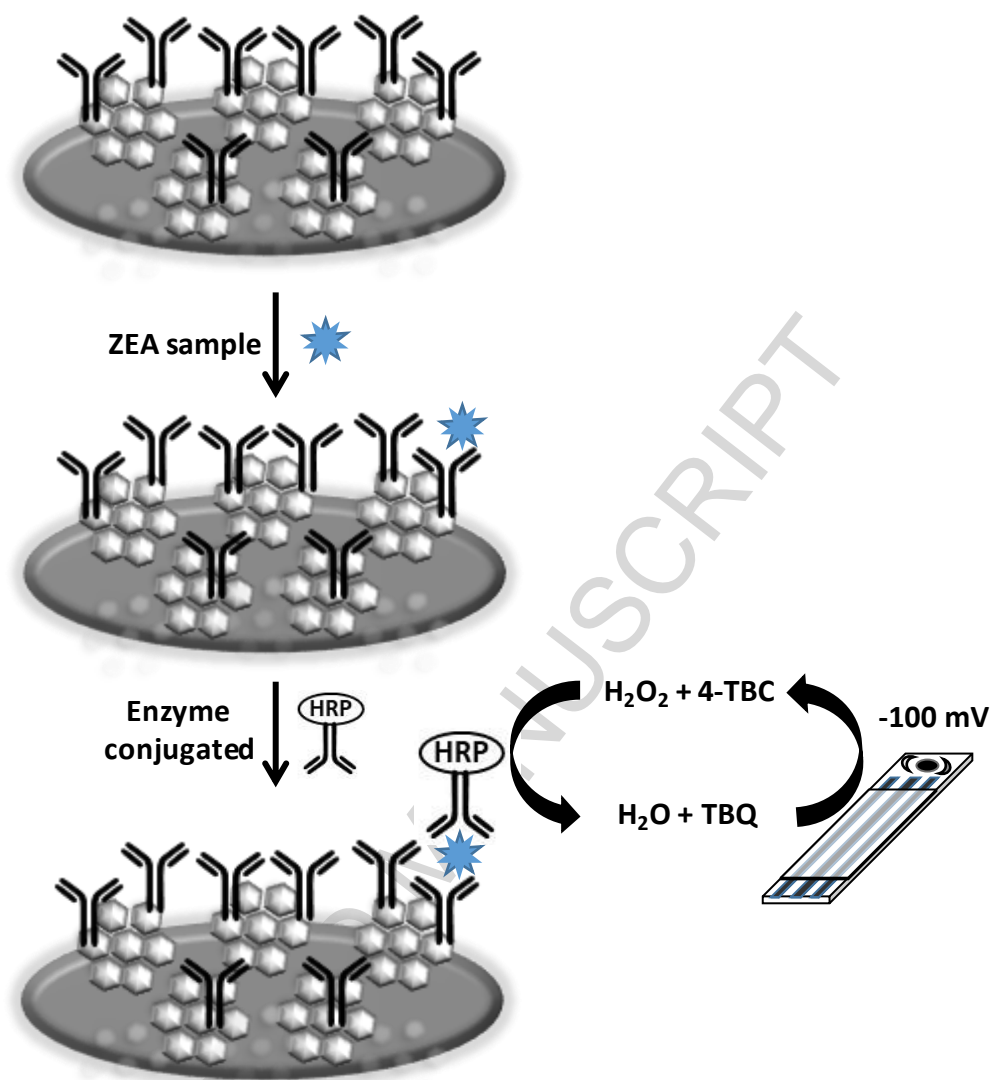
**Fig. 3.** Electrochemical characterization of the different modified electrodes. CVs were performed in 1 mmol L<sup>-1</sup> K<sub>3</sub>[Fe(CN)<sub>6</sub>]/K<sub>4</sub>[Fe(CN)<sub>6</sub>] in 0.1 mol L<sup>-1</sup> KCl (pH 6.50) solution from -300 mV to +900 mV at a 75 mV s<sup>-1</sup> scan rate.

**Fig. 4.** Optimization of experimental conditions. a) pH of phosphate-citrate buffer, b) HRP-anti-ZEA concentration, c) H<sub>2</sub>O<sub>2</sub> concentration, and d) 4-TBC concentration.

**Fig. 5.** Calibration curve for ZEA from 1.88 to 45 ng mL<sup>-1</sup>,  $\Delta I \text{ (nA)} = 15.18 + 19.33 [\text{ZEA}]$  (ng mL<sup>-1</sup>), with a correlation coefficient of 0.998, and the detection limit is 0.57 ng mL<sup>-1</sup>.



Scheme 1



Scheme 2



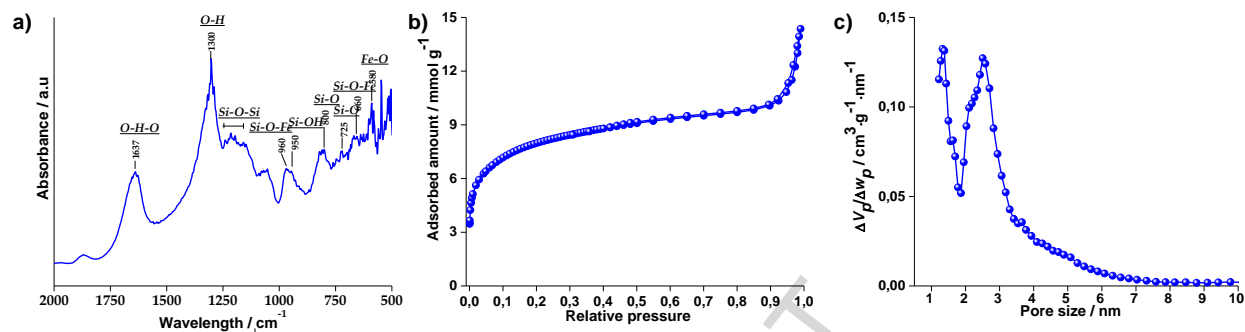
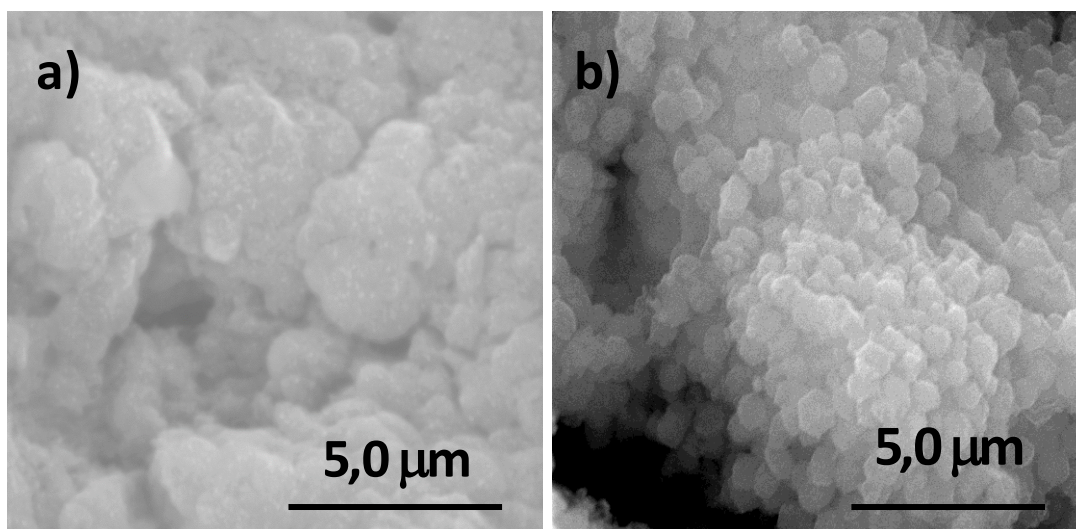
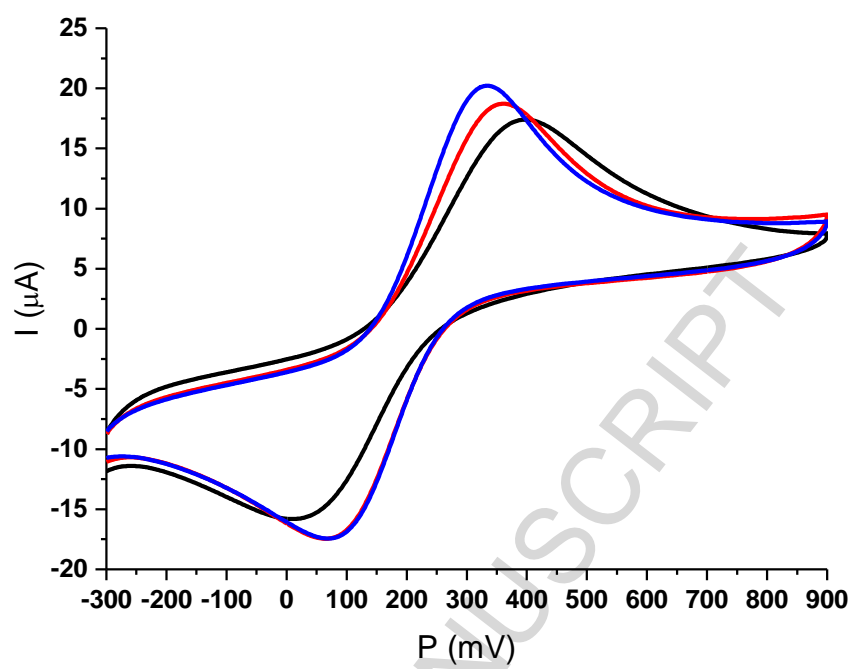


Fig. 1



**Fig. 2**

**Fig. 3**

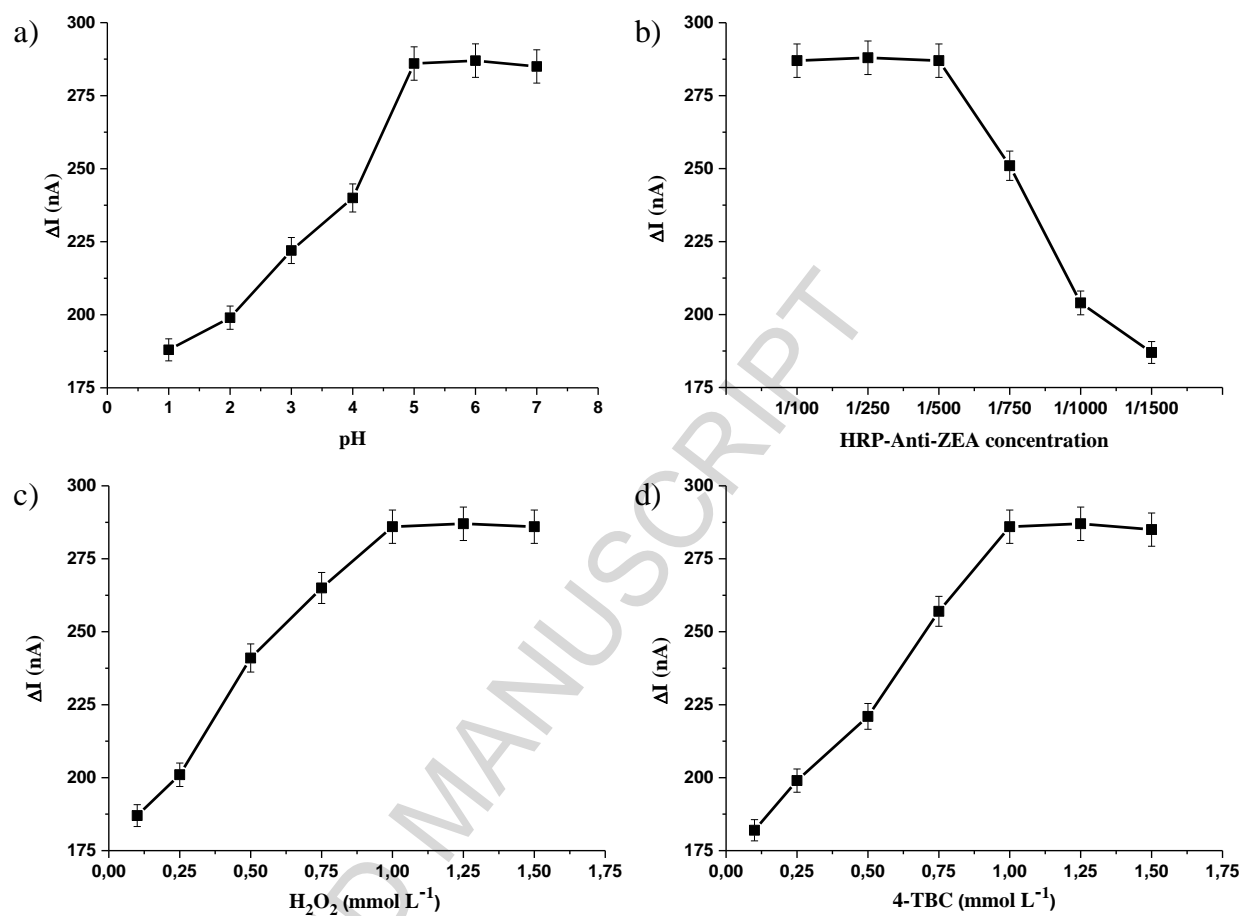


Fig. 4

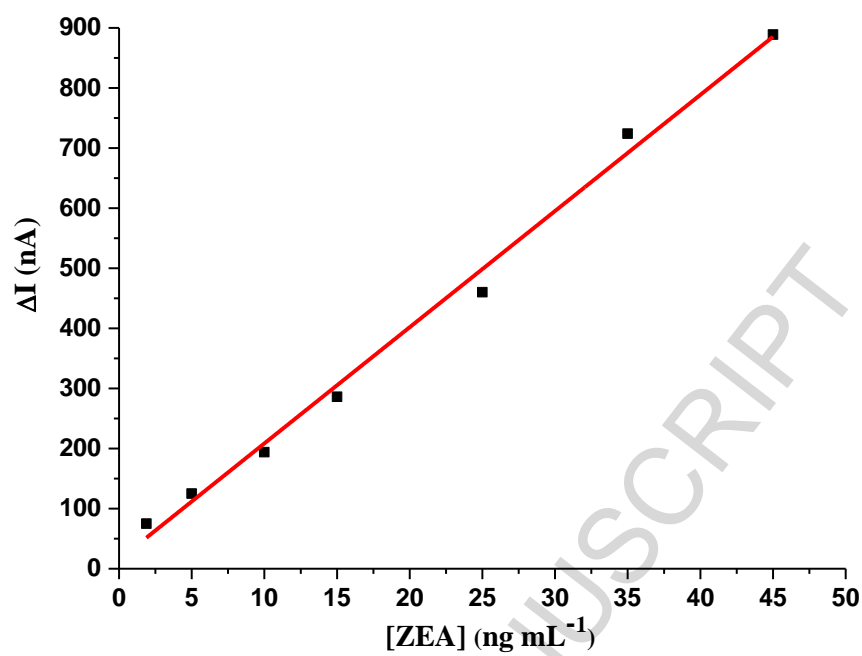


Fig. 5

**Table 1.** Comparison between the electrochemical immunosensor and ELISA for ZEA quantification.

Samples <sup>a</sup>	Methods	
	EI <sup>b</sup>	ELISA <sup>c</sup>
S 1	3.15 <sup>d</sup> ± 0.11 <sup>e</sup>	3.81 ± 0.14
S 2	9.21 ± 0.21	9.32 ± 0.29
S 3	19.46 ± 0.48	19.97 ± 0.31
S 4	35.87 ± 0.37	35.18 ± 0.54
S C	-	-

<sup>a</sup> *A. cruentus* seeds samples (S 1-4), and the negative control sample (S Control)

<sup>b</sup> Electrochemical immunosensor

<sup>c</sup> Enzyme immunoassay

<sup>d</sup> ng mL<sup>-1</sup>

<sup>e</sup> Mean of five determinations ± S.D.

**Table 2.** Comparison of recently immunosensors for ZEA determination.

Method	Materials	Sample	LOD <sup>a</sup>	Reference
Amperometry	Multiwall carbon nanotubes	Corn	0.77	[33]
Fluorescence	Pore glass-Prot A	Corn	0.007	[34]
Amperometry	Magnetic microparticles	Feedstuffs	0.41	[35]
Amperometry	Paramagnetic beads	Baby food	0.007	[36]
Amperometry	MCM-41-Fe <sub>2</sub> O <sub>3</sub>	Seeds	0.57	This method

<sup>a</sup> (ng mL<sup>-1</sup>)

### Highlights

- We describe the first electrochemical immunosensor for ZEA determination in *Amaranthus cruentus* seeds.
- The device is based on a screen printed carbon electrode (SPCE) modified with amino mesoporous silica (MCM-41) synthesized with  $\text{Fe}_2\text{O}_3$  *in situ*.
- Mesoporous material enlarges the surface available for anti-ZEA antibodies immobilization.
- The method exhibits good selectivity, stability and reproducibility for ZEA detection to ensure food safety, as well as consumer's health.